

Investigating the Potential and Limitations of Cell Spacing Adjustment for Optimized Air-Based Battery Thermal Management Systems

Amin Moosavi*, Anna-Lena Ljung, Staffan Lundström

Division of Fluid Mechanics, Department of Engineering Sciences and Mathematics, Luleå University of Technology, 971 87 Luleå, Sweden

(*Corresponding Author: amin.moosavi@ltu.se)

ABSTRACT

A reliable battery thermal management system plays a crucial role in the safe, efficient, and long-term operation of a high-performance lithium battery system. This study evaluates the temperature rise, pressure drop, capacity loss, and cyclical cost of an air-cooled battery system consisting of 90 cylindrical battery cells placed in a staggered arrangement in the module. The effect of spacing between the adjacent cells and inflow velocity is investigated for the battery system operating at high charge/discharge rates of 3C and 5C. The results demonstrate that the hybrid model, which consists of the battery life model integrated with the simplified modeling approach for the thermal evaluation of battery packs, provides a cost-effective tool for multi-objective analysis and optimization of air-cooled battery packages. The results reveal that the air-based cooling system has the potential to fulfill the safety standards in all studied cases, and employing battery modules with larger cell spacing at a constant inflow velocity may reduce the maximum temperature, pressure drop, and cyclical cost by up to 2.14%, 93.36%, and 35.69%, respectively, while extending the lifespan of the battery system by up to 55.45%. However, it is found that the air-based cooling system approaches its limit of thermal performance at high inflow velocities. A novel index (MCR index) is proposed in this paper to characterize the limitations associated with adjusting cell spacing for air-based battery cooling systems. It is observed that for systems with an MCR index beyond 600, the effect of cell spacing on thermal performance becomes negligible. This can be used as a useful guideline for optimizing air-based battery thermal management systems or integrating them with other cooling methods.

Keywords: battery thermal management system, cylindrical lithium battery, air-cooled system, spacing effect, simplified modeling approach, cyclical cost

1. INTRODUCTION

The global demand for lithium is growing with the trend toward the electrification of systems. However, there are some serious problems against the widespread use of lithium-ion batteries, such as safety, cost, lifespan, energy density, and environmental impact which are all somehow connected to the temperature sensitivity issue in lithium batteries. This issue necessitates the requirement of an auxiliary cooling system, known as a battery thermal management system, for the efficient operation of battery packages. There are different types of battery thermal management systems, each with its own strengths and drawbacks; nonetheless, they all have the same primary task of regulating the temperature of battery cells under various operational conditions.

In comparison to the other battery cooling methods, air-based battery thermal management systems have received considerable attention due to their low weight, simple design, and low cost, easy maintenance, and low environmental impact. Although passive air cooling can be sufficient for the efficient operation of battery packages at a low charging/discharging rate of 0.5 C [1], it is observed that forced convection is required to mitigate temperature rise at high C rates [2]. The performance of forced air-cooling systems depends on several factors, including flow direction, the number and placement of vents, the arrangement and spacing of the battery cells, and so on. Hence, numerous studies have been done to understand and investigate the effect of these factors on the performance of battery thermal management systems based on forced air cooling [3]. According to the study by Zhang et al. [4], the layout,

which consists of a single inlet on top and outlets on four sides of the battery package, can reduce the maximum temperature and the maximum temperature difference in the battery package by 16.4% and 48.7%, respectively. Regarding the battery arrangement, it has been found that the line-up arrangement provides superior thermal performance in comparison to square-type and ring-type battery arrangements [5]. Moreover, Saechen et al. [2] determined that the staggered arrangement of the cells in compact air-cooled battery packages could be the optimal choice in terms of maximum temperature, temperature distribution, and power consumption. Zhao et al. [6] assessed the gradient vertical spacing of the battery cells against a regular rectangular cell arrangement. The results indicate that the gradient vertical spacing of the cells reduces thermal concerns at the expense of increasing pressure drop and an insignificant superiority in space utilization. Shen et al. [7] demonstrated that 19° rotation of the batteries along the inlet/outlet direction for the z-shaped battery air-based battery thermal management systems decreases the maximum temperature and temperature difference by 10.5% and 23.9%, respectively. The research by Sahin et al. [8] indicates that employing delta winglet baffles in air-cooled battery packages brings down the maximum temperature and temperature difference by up to 2% and 15% while leading to 44% more power consumption.

Despite the advantages of air-cooled systems, their efficiency is limited by the low thermal conductivity of air as a cooling medium. Hence, some scholars have combined the air-based method with other cooling methods to enhance the overall performance of the system. Singh et al. [9] demonstrated that adding 1 [mm] layer of n-octadecane as phase change material (PCM) on the surface of cylindrical batteries can significantly improve the thermal performance of the cooling system at high charging/discharging rates. The mist cooling system proposed by Saw et al. [10] in comparison to conventional dry air-cooling systems showed up to a 45% better thermal performance. The hybrid cooling system developed by Xin et al. [11] was designed to regulate temperature rise in the battery cells by using liquid-cooled heat conducting blocks and an air-cooling system to manage temperature distribution.

As shown, the majority of the research on battery thermal management systems revolves around achieving thermal safety requirements by changing geometrical parameters. However, for some applications, particularly stationary lithium batteries, hybrid electric vehicles, small electric vehicles, and even hybrid-electric aircraft

at low power periods [12], the safety concerns have almost been addressed, and the challenging issues are the efficiency of the cooling system, degradation rate, cycle life, and costs. Unfortunately, only a few studies [13,14] have taken these concerns into account while designing their battery thermal management system.

By considering the gap in the field, this paper conducts a multi-objective analysis of an air-based battery thermal management system. The study is based on the simplified modeling approach which enables time-efficient parametric assessment of the battery module. The effect of varying charging/discharging rate, inlet velocity, and cell spacing on the operation of an air-cooled battery module is evaluated by taking maximum temperature, temperature difference, pressure drop, capacity loss, and cyclical cost into consideration. The findings provide a roadmap for the optimal designing of air-based battery thermal management systems based on the needs and limitations.

2. PHYSICAL MODEL

The battery package consists of 270 cylindrical lithium battery cells distributed in three modules to suit the requirements of a hybrid electric vehicle. The cylindrical battery cells employed for this study are 26650 LFP lithium batteries, the specifications of which are listed in Table 1. The battery cells are placed in a staggered arrangement with an equal gap distance between the two adjacent cells. The schematic view of the battery module is shown in Fig. 1.

Table 1: Specifications of 26650 LFP battery cell [14, 15].

| <i>Parameter</i> | <i>Unit</i> | <i>Value</i> |
|------------------------------------|-------------------------|--------------|
| <i>Diameter</i> | <i>mm</i> | <i>26</i> |
| <i>Height</i> | <i>mm</i> | <i>65</i> |
| <i>Density</i> | <i>kg/m³</i> | <i>2047</i> |
| <i>Nominal voltage</i> | <i>V</i> | <i>3.3</i> |
| <i>Nominal capacity</i> | <i>A.h</i> | <i>2.3</i> |
| <i>Internal resistance</i> | <i>mΩ</i> | <i>8</i> |
| <i>Specific heat capacity</i> | <i>J/(kg K)</i> | <i>1100</i> |
| <i>Radial thermal conductivity</i> | <i>W/(m K)</i> | <i>1.18</i> |
| <i>Axial thermal conductivity</i> | <i>W/(m K)</i> | <i>39.49</i> |

3. MODELLING APPROACH

3.1 Thermal model for battery module

Given the large-scale and transient behavior of battery packages, the integrated simulation of the battery cooling system could be quite challenging, particularly in terms of computing cost. Hence, in this

work, we have implemented a simplified modeling approach described by Moosavi et al. [15] to efficiently predict the thermal behavior of the battery module in different operating conditions. The simplified modeling approach divides the integrated model into three discrete parts: (1) an analytical model based on the integral transform technique for the prediction of temperature field within the cylindrical battery cells [16], (2) a CFD model to predict heat transfer rate in the periodic flow region [17], and (3) a series of approximate equations to estimate row-to-row thermal evolution along the cooling system, all of which are linked together via the heat transfer coefficient. Basically, the process starts with the thermal evaluation of flow in the periodic flow region using the CFD model. Then, a series of equations are used to calculate the heat transfer rate and reference flow temperature for each row along the battery pack. Finally, all the data is plugged into the analytical model that predicts the temperature field for each cell under various operating conditions. This technique allows efficient analysis of the battery cooling system in different working conditions with the desired order of accuracy for each sub-model.

A similar approach is employed for this work; however, the CFD model is replaced with the Gnielinski correlation [18] to determine the average heat transfer rate for different geometrical and flow conditions, which may be expressed as follows:

$$Nu = f_{A,stag} \left(0.3 + \sqrt{Nu_{lam}^2 + Nu_{turb}^2} \right) \quad (1)$$

with

$$f_{A,stag} = 1 + \frac{2}{3b} \quad (2)$$

$$Nu_{lam} = 0.664 \sqrt{Re_{\psi}} \sqrt[3]{Pr} \quad (3)$$

$$Nu_{turb} = \frac{0.037 Re_{\psi}^{0.8}}{1 + 2.443 Re_{\psi}^{0.1} \left(Pr^{\frac{2}{3}} - 1 \right)} \quad (4)$$

and

$$Re_{\psi} = \frac{\rho v_{in} l}{\mu \Psi}. \quad (5)$$

The l , Ψ , a , and b in the above equations represents streamed tube length, void fraction, transverse pitch ratio, and longitudinal pitch ratio, respectively, as defined in [18].

3.2 Pressure drop model for battery module

The pressure drop of airflow through the battery cells can be derived by [19]

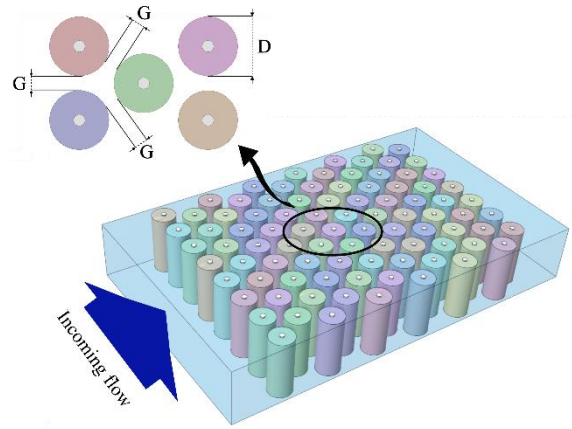


Figure 1: Schematic view of the battery module.

$$\Delta P = \xi n_{MR} \frac{\rho V_g^2}{2} \quad (6)$$

where ξ , n_{MR} , and V_g represent the drag coefficient, the number of resistances in the flow direction, and the velocity in the shortest gap between the cells. To calculate the drag coefficient in the battery module, we employed the correlation proposed by Gaddis [19]:

$$\xi = \xi_{lam} + \xi_{turb} F_v \quad (7)$$

with

$$F_v = 1 - \exp\left(-\frac{Re_g + 200}{1000}\right) \quad (8)$$

$$\xi_{lam} = \frac{1}{Re_g} \left(\frac{280\pi[(b^{0.5} - 0.6)^2 + 0.75]}{(4ab - \pi)a^{0.6}} \right) \quad (9)$$

$$\xi_{turb} = \frac{1}{Re_g^{0.25}} \left(2.5 + \frac{1.2}{(a - 0.85)^{1.08}} + 0.4 \left(\frac{b}{a} - 1 \right)^3 - 0.01 \left(\frac{a}{b} - 1 \right)^3 \right). \quad (10)$$

In Eqs. (8)-(10), Re_g corresponds to $\frac{\rho v_g D}{\mu}$, where D and v_g represent the diameter of a cell and the velocity in the shortest gap between the adjacent battery cells, respectively.

3.3 Battery life model

The lifetime of battery cells is evaluated using the life model proposed by Wang et al. [20]. The model is an empirical model that is developed based on the capacity loss of 26650 LFP battery cells during each cycle of charging/discharging. Hence, the percentage of capacity loss after each cycle can be calculated as follows:

$$Q_{loss} = B \cdot \exp\left(\frac{-31700 + (370.3 \times C_{rate})}{R_{gas} T}\right) A_h^{0.55}. \quad (11)$$

R_{gas} , T , C_{rate} , and A_h in Eq. (12) denotes the gas constant (equals to 8.314 [J/ (mol² K)]), the average

surface temperature of the battery cell, the charging/discharging rate, and total A.h throughput, respectively. The coefficient B corresponds to C_{rate} , and can be determined using the chart below.

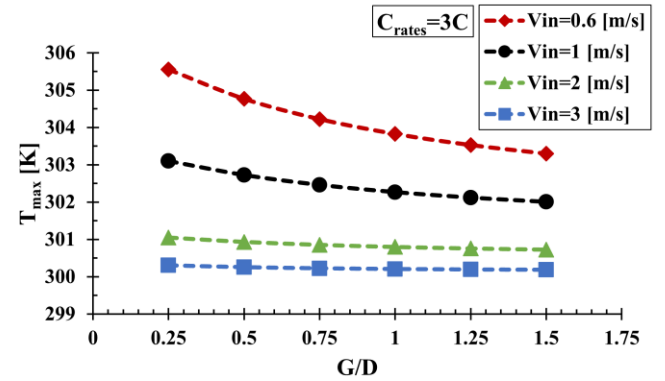
Table 2: Values of coefficient B in Eq. (11).

| C_{rate} | 0.5 | 2 | 6 | 10 |
|------------|-------|-------|-------|-------|
| B | 31630 | 21681 | 12934 | 15512 |

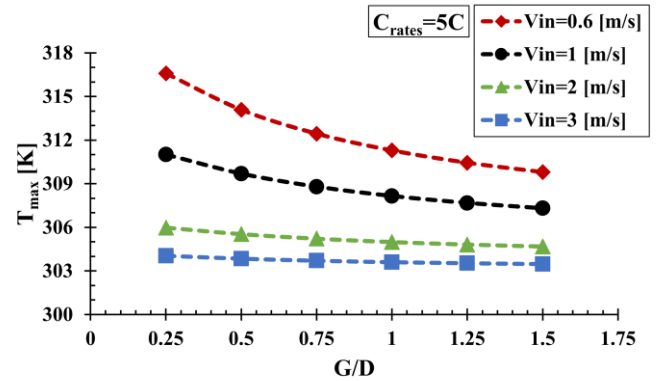
4. RESULTS AND DISCUSSION

In this work, 90 cylindrical battery cells per module are connected in series and it is expected that a fan blows air through the battery cells at a constant inlet velocity (V_{in}) and constant temperature of 25 °C. According to the study conducted by Zolot et al. [21], the average power profile for a hybrid vehicle under the US06 driving cycle is 3.2 kW. This power profile corresponds to a charging/discharging rate of 1.56 C for the battery pack presented in this work. Nonetheless, it is assumed that the battery module goes through two different charging/discharging rates of 3C and 5C to investigate the system’s performance in extreme working conditions and standardize it with rates used in the other references.

As stated earlier, air-based battery thermal management systems offer multiple advantages over alternative cooling systems, including lightweight, no leakage problems, ease of maintenance, and low cost. However, their performance may be challenged in extreme working conditions due to the low thermal conductivity of the coolant (air). Hence, careful evaluation of design considerations plays a major role in the efficient operation of air-based battery cooling systems. In the following, thermal performance, parasitic power consumption, capacity loss level, and cyclic cost are evaluated in two different charging/discharging conditions for the cooling system with variable gap distance to cell diameter (G/D) and air inlet velocities. The maximum temperature for the battery module with variable cell spacing (G/D) and inlet velocity (V_{in}) is shown in Figs. 2(a) and 2(b), respectively, at 3C and 5C charging/discharging rates. The results indicate that the air-based cooling system can secure the safe operation of the battery module even at a high charging/discharging rate by maintaining the maximum temperature below 50°C. However, the temperature rise at 5C compared to the 3C charging/discharging rate is significantly closer to the battery safety limits, particularly at low inlet velocities of 0.6 and 1 [m/s]. Generally, it can be stated that first, the cooling system



(a)



(b)

Figure 2: Maximum temperature at charging/discharging rate of (a) 3C and (b) 5C for varying inflow velocities and gap distances between the cells.

with a higher air inlet velocity can better mitigate the temperature rise in the module, and second, the battery layout with a wider distance between the adjacent cells has better cooling performance. Although the first statement is connected to the enhanced Nusselt number

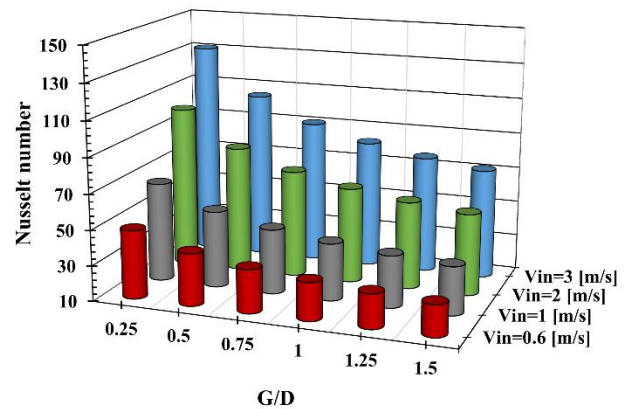


Figure 3: The average Nusselt number of the battery module at different inflow velocities and gap distances between neighboring cells.

for the battery module with a higher air inlet velocity, as shown in Fig. 3, the second statement cannot be justified by the Nusselt number changing pattern in varied cell spacing. To describe this behavior, it should be noted that the Nusselt number indicates the potential of the surface for heat transfer rather than the quantity of heat transfer. Hence, by decreasing the gap distance between the cells at constant inlet velocity, even if the surface of the cells may better transfer the heat owing to the enhanced Nusselt number, the quantity of heat transfer is reduced due to lower air intake mass flow rate, resulting in temperature rise within the battery cells.

Moreover, the results in Fig. 2 show that varying the distance between the adjacent cells has no significant effect on the maximum temperature at high flow rates despite the changes in Nusselt number. To characterize this behavior, the module cooling resistance (MCR) index is introduced as follows:

$$MCR = \left(\frac{3600}{C_{rate}} \right) \left(\frac{hA + \dot{m}c_{p,f}}{\rho_b \nabla_b c_{p,b}} \right). \quad (12)$$

In Eq. (12), h , A , \dot{m} , $c_{p,f}$, ρ_b , ∇_b , and $c_{p,b}$ reflect the average heat transfer coefficient of the module, surface area for heat transfer, inlet mass flow rate, the specific heat capacity of the fluid, density, volume, and specific heat capacity of the battery cell, respectively. Basically, the MCR index evaluates the balance between the potential of the convection-based cooling system for heat dissipation and the resistance of the battery cells against heat removal. In Eq. (12), hA [W/K] denotes the rate of heat dissipation from the cooling surface if the surface and reference fluid temperatures differ by one Kelvin. The term $\dot{m}c_{p,f}$ [W/K] demonstrates the rate of heat that might be transferred to the cooling medium (air) as its temperature rises by one Kelvin. $\rho_b \nabla_b c_{p,b}$ [J/k] indicates the amount of heat that might be stored in a battery cell if its temperature rises by one Kelvin during charging/discharging time ($3600/C_{rate}$ [s]). In general, a lower MCR value indicates that the potential of the cooling system for heat dissipation compared to the resistance of the battery cells for heat removal is insignificant. In this condition, any modifications to enhance the cooling performance of the system may result in a significant improvement. The MCR values in Fig. 4, shown for the studied cases at the 5C charging/discharging rate, help to explain the unchanged trend of maximum temperature curves at high inlet velocities as seen in Fig. 2.

According to Fig. 4, reduced air inlet velocity and gap distance between the adjacent cells lead to a lower MCR

value. This indicates that for these cases with lower MCR values, the system's cooling potential and the heat accumulation potential of the cells are closer to equilibrium. Therefore, any changes disturbing this

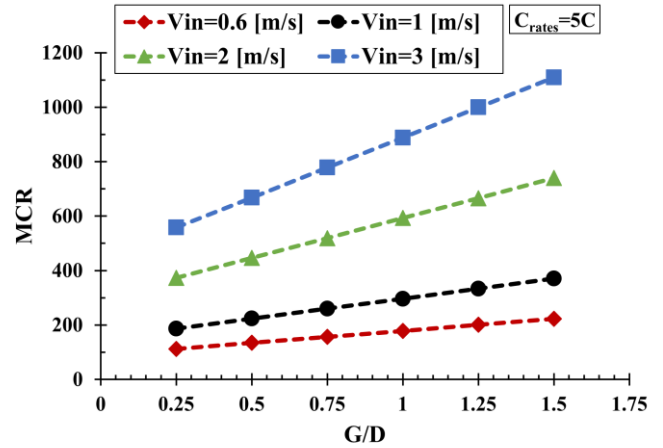


Figure 4: MCR values for varied inlet velocities and cell spacing at a charging/discharging rate of 5C.

equilibrium have a greater impact on thermal performance. However, in the cases with high MCR values, the cooling performance far exceeds the resistance of the cells for heat removal, implying that a substantial modification is required to improve the cooling performance. In other words, the battery cooling system is approaching its limitation and resists any further modification. In this study, we observed that the resistance against modification arises at MCR levels close to 600. Overall, the MCR index may be a helpful index to characterize the limitations of the enhancement methods used for improving the thermal performance of battery thermal management systems.

Fig. 5 displays the change of pressure drop in the battery module by varying the distance between the

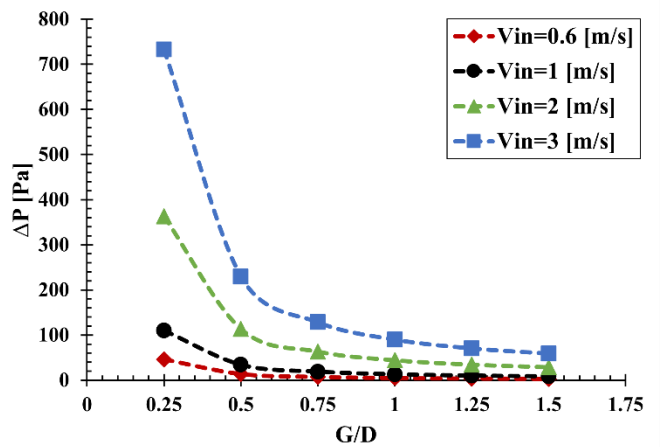


Figure 5: The pressure drop across the battery module at different inlet velocities and cell spacing.

neighboring cells and the inlet velocity to the system. The results indicate that, even though increasing inflow velocity improves temperature management in the module, it imposes a considerable pressure drop on the system, especially in narrow spacing layouts, which can be restricted by increasing the gap distance between the cells. The rise in pressure drop increases the power requirements of the cooling system, which consequently may influence overall efficiency, space utilization, noise control, and cost of the system.

Along with the concerns related to the thermal performance and power efficiency of the battery cooling system, the lifetime and cost are additional aspects that should be considered in the overall evaluation of a battery system, particularly if the battery system fulfills the safety standards. Hence, the cyclical cost index proposed by Chen et al. [13] is employed in the evaluation of the system for different designs and working conditions. The cyclical cost index evaluates the costs associated with manufacturing and parasitic power consumption in the system while also addressing the number of cycles the battery system can operate efficiently, which is closely tied to the operating parameters and cooling condition of the system. In Fig. 6, the capacity loss of the battery at a 5C charging/discharging rate and an inflow velocity of 0.6 [m/s] is shown for different gap spacing. It is evident that the battery reaches the end of its life (20% capacity loss) in fewer cycles by narrowing the gap between the cells as a consequence of poor cooling conditions.

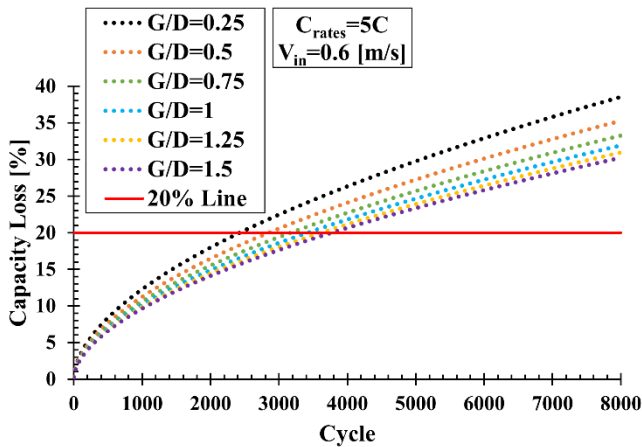


Figure 6: The effect of cell spacing on battery capacity loss.

The cyclical cost index for a hybrid vehicle might be expressed as follows:

$$\delta = \frac{\tau_b C_{nom}^M + \beta N_{eof} Q_p}{N_{eof}} \quad (13)$$

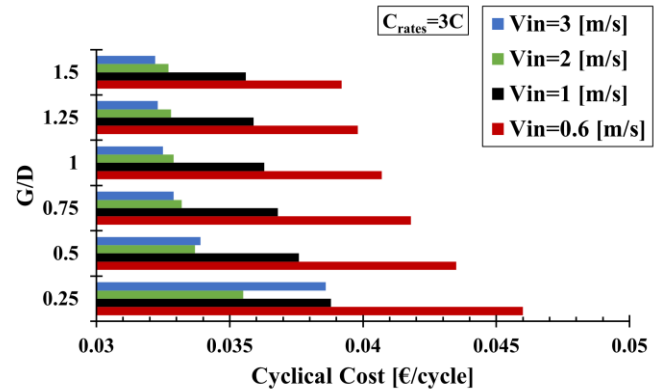
with

$$\beta = \frac{\tau_D}{H_D \eta_{PT}}. \quad (14)$$

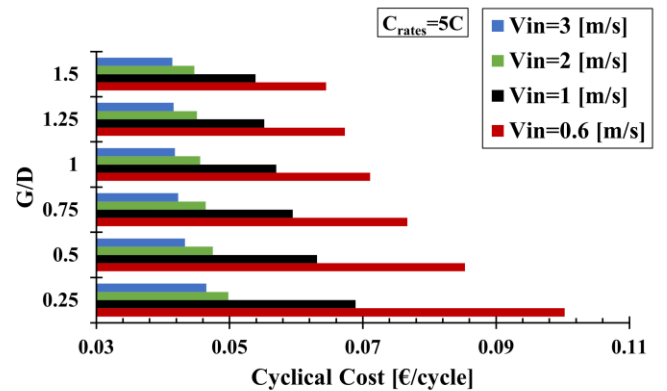
In the above equations, δ , C_{nom}^M , N_{eof} , and Q_p denotes cyclical cost, nominal capacity of the battery module, number of cycles until the end of life, and parasitic power consumption, respectively. The remaining required parameters can be found in Table 3. The cyclical cost for different cases is shown in Fig. 7.

Table 3: Some parameters for cyclical cost evaluation.

| Parameter | Unit | Value |
|-----------------------------------|-------|-------|
| Battery price [22] | €/kWh | 356 |
| Fuel price | €/L | 1.914 |
| Diesel lower heating value [13] | MJ/L | 38.6 |
| Hybrid powertrain efficiency [13] | % | 30.1 |



(a)



(b)

Figure 7: The cyclical cost evaluation of the battery module at different inflow velocities and cell spacing.

As seen in Fig. 7(b), the cyclical cost, at a high charge/discharge rate of 5C, increases by reducing the

inflow velocity and distance between the nearby battery cells. Despite the smaller pressure drop at low inflow velocities, the increased battery degradation owing to poor thermal management has significantly reduced the efficient lifetime of the battery and consequently increased the overall cyclical cost. However, at a lower charge/discharge rate of 3C, the cyclical cost variation trend seems dissimilar for the compact layouts (see Fig. 7(a), $G/D= 0.25$, and 0.5). It is because the extended lifespan of the battery module at a high inflow velocity of 3 [m/s] (owing to improved thermal management) is no longer worth the significant power consumption cost to overcome pressure drop. This behavior highlights the importance of multi-objective studies in the optimal design of air-based battery thermal management systems, particularly in low- or medium-charging/discharging applications.

5. CONCLUSIONS

In this work, an air-based battery thermal management system is investigated using a simplified modeling approach. A multi-objective analysis is performed to study how the cell spacing, inflow velocity, and charge/discharge rate affect temperature rise, pressure drop, capacity loss, and cyclical cost in an air-cooled battery system. The results indicate that even at a high charge/discharge rate of 5C with a low inflow velocity of 0.6 [m/s], the air-based battery thermal management system can effectively maintain the temperature rise within the safety limits. Furthermore, the study demonstrates that increasing the gap distance between the adjacent cells at constant inflow velocity reduces the maximum temperature and pressure drop by up to 2.14% and 93.36%, respectively. However, the improved cooling performance due to the adjusted cell spacing becomes constrained at high inflow velocities, which can be explained using the proposed MCR index. When the MCR value exceeds 600, the system approaches its limitations, and a more significant enhancement method is required to change the thermal performance of the system. Despite the low or limited effect of battery layout, it is found that increasing the gap between the nearby cells can extend the lifetime of the battery by up to 55.45%. This lifetime extension consequently affects the cyclical cost of the battery module, which may be reduced by up to 35.69% at constant inflow velocity. In addition, the results reveal that cyclical cost evaluation might be essential for optimizing battery systems operating at low charge/discharge rates, where the optimal design may

not correlate with findings from thermal and power evaluation.

ACKNOWLEDGEMENT

This work was funded by and performed within the framework of the StandUp for Energy and Green Transition North.

DECLARATION OF INTEREST STATEMENT

The authors declare that they have no known competing financial interests or personal relationships that could have appeared to influence the work reported in this paper. All authors read and approved the final manuscript.

REFERENCE

- [1] Yu, X., Lu, Z., Zhang, L., Wei, L., Cui, X., & Jin, L. (2019). Experimental study on transient thermal characteristics of stagger-arranged lithium-ion battery pack with air cooling strategy. *Int J Heat Mass Transf*, *143*, 118576.
- [2] Saechan, P., & Dhuchakallaya, I. (2022). Numerical investigation of air cooling system for a densely packed battery to enhance the cooling performance through cell arrangement strategy. *Int J Energy Res*, *46*(14), 20670-20684.
- [3] Zhao, G., Wang, X., Negnevitsky, M., & Zhang, H. (2021). A review of air-cooling battery thermal management systems for electric and hybrid electric vehicles. *J Power Sources*, *501*, 230001.
- [4] Zhang, F., Wang, P., & Yi, M. (2021). Design optimization of forced air-cooled lithium-ion battery module based on multi-vents. *J Energy Storage*, *40*, 102781.
- [5] Zhang, Y., Song, X., Ma, C., Hao, D., & Chen, Y. (2020). Effects of the structure arrangement and spacing on the thermal characteristics of Li-ion battery pack at various discharge rates. *Appl Therm Eng*, *165*, 114610.
- [6] Zhao, G., Wang, X., & Negnevitsky, M. (2021). A study of variable cell spacings to the heat transfer efficiency of air-cooling battery thermal management system. *Appl Sci*, *11*(23), 11155.
- [7] Shen, X., Cai, T., He, C., Yang, Y., & Chen, M. (2023). Thermal analysis of modified Z-shaped air-cooled battery thermal management system for electric vehicles. *J Energy Storage*, *58*, 106356.
- [8] Sahin, R. C., Gocmen, S., & Cetkin, E. (2022). Thermal management system for air-cooled battery packs with flow-disturbing structures. *J Power Sources*, *551*, 232214.
- [9] Singh, L. K., Gupta, A. K., & Sharma, A. K. (2022). Hybrid thermal management system for a lithium-ion battery module: Effect of cell arrangement, discharge rate, phase change material thickness and air velocity. *J Energy Storage*, *52*, 104907.
- [10] Saw, L. H., Poon, H. M., San Thiam, H., Cai, Z., Chong, W. T., Pambudi, N. A., & King, Y. J. (2018). Novel

thermal management system using mist cooling for lithium-ion battery packs. *Appl energy*, 223, 146-158.

[11] Xin, S., Wang, C., & Xi, H. (2023). Thermal management scheme and optimization of cylindrical lithium-ion battery pack based on air cooling and liquid cooling. *Appl Therm Eng*, 224, 120100.

[12] Coutinho, M., Bento, D., Souza, A., Cruz, R., Afonso, F., Lau, F., ... & da Silva, C. R. (2023). A review on the recent developments in thermal management systems for hybrid-electric aircraft. *Appl Therm Eng*, 120427.

[13] Chen, F., Huang, R., Wang, C., Yu, X., Liu, H., Wu, Q., Bhagat, R. (2020). Air and PCM cooling for battery thermal management considering battery cycle life. *Appl Therm Eng*, 173, 115154.

[14] Li, W., Wang, N., Garg, A., & Gao, L. (2023). Multi-objective optimization of an air cooling battery thermal management system considering battery degradation and parasitic power loss. *J Energy Storage*, 58, 106382.

[15] Moosavi, A., Ljung, A. L., & Lundström, T. S. (2023). A study on the effect of cell spacing in large-scale air-cooled battery thermal management systems using a novel modeling approach. *J Energy Storage*, 72, 108418.

[16] Moosavi, A., Ljung, A. L., Lundström, T. S. (2021). Design considerations to prevent thermal hazards in cylindrical lithium-ion batteries: An analytical study. *J Energy Storage*, 38, 102525.

[17] Moosavi, A., Ljung, A. L., Lundström, T. S. (2023). A comparative study on thermo-fluid characteristics of free and wall-bounded cross-flow heat exchangers. *Therm Sci Eng Prog*, 40, 101746.

[18] Gnielinski, V. (2010). Heat transfer in cross flow around single rows of tubes and through tube bundles. In VDI Heat Atlas. 2nd ed., Berlin: Springer, 725-729.

[19] Gaddis, E. S. (2010). Pressure drop of tube bundles in cross flow. In: VDI Heat Atlas. 2nd ed., Berlin: Springer, 1076-1091.

[20] Wang, J., Liu, P., Hicks-Garner, J., Sherman, E., Soukiazian, S., Verbrugge, M., ... & Finamore, P. (2011). Cycle-life model for graphite-LiFePO₄ cells. *J power sources*, 196(8), 3942-3948.

[21] Zolot, M., Pesaran, A. A., Mihalic, M. (2002). *Thermal evaluation of Toyota Prius battery pack* (No. 2002-01-1962). SAE Technical paper.

[22] Patry, G., Romagny, A., Martinet, S., & Froelich, D. (2015). Cost modeling of lithium-ion battery cells for automotive applications. *Energy Sci Eng*, 3(1), 71-82.